

1. SPR screening of synthetic peptides from the GH loop of FMDV

1.0 Introduction

The first objective of the present work was the study of the applicability of SPR biosensors¹ to kinetically characterise the interactions between peptides related to viral antigenic sites and relevant monoclonal antibodies². In particular, the research was focused on the interactions between anti-FMDV mAbs and synthetic peptides reproducing an immunodominant region of FMDV (antigenic site A, residues 136-150 of envelope protein VP1, isolate C-S8c1)³⁻⁵ to examine the main structural features involved in the recognition of this site by neutralising antibodies. Synthetic peptides reproducing different mutations at this site are particularly useful in identifying residues involved in recognition or escape events^{6,7}. Given the large number of such peptides and the relatively small number of relevant mAbs, the most productive approach would seem to be mAb immobilisation and analysis of the peptides as soluble analytes. However, a limitation of the SPR technique is that interactions between low molecular weight (<5 kDa^A) analytes and their immobilised binding partners cannot, in principle, be studied directly since the increase in mass on the sensor chip is too small to provide reliable data⁸. Not only small responses are a problem, but also bulk refractive index effects together with non-specific

binding and mass-transport limitations can affect true binding kinetics, particularly in the direct detection of small analytes. A possible way to circumvent detection problems associated with small analytes is to use a competitive kinetic analysis with a high molecular weight analyte for the same ligand binding site⁹. However, this approach was not initially feasible, since a high molecular weight representative of antigenic site A, *e. g.*, capsid protein VP1 of

FMDV, was unavailable. In view of this, it was decided to work with immobilised mAb and address the difficulties associated with the small size (≈ 1.6 kDa) of the peptide analytes.

A 1:1 bimolecular interaction kinetics is to be expected for peptide-antibody interaction, if both antigen-binding fragments are considered independent and equivalent (Fig. 1.1)¹⁰.

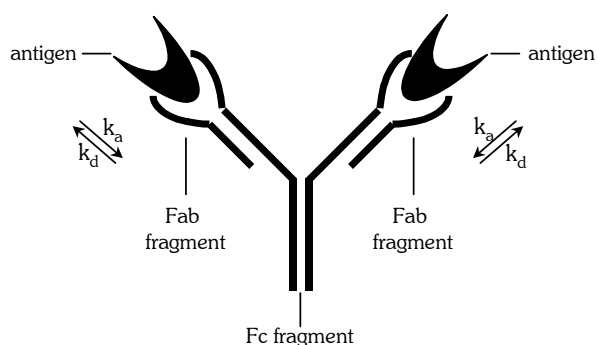


Figure 1. 1 Representation of an antigen – antibody interaction; Fab stands for antigen-binding fragment and Fc for crystallisable fragment.

^A The experimental work described in the present thesis has been carried out using a BIACORE 1000 instrument. Since this work was completed, improved versions of the BIACore instrumentation with higher sensitivity (BIACORE 2000, 3000, X...) have been commercialised.

1.1 Optimisation of the experimental set-up

Antigenic site A of FMDV C-S8c1 contains several distinct, overlapping, B-cell epitopes and is located in the GH loop (residues 136 to 150) of the envelope protein VP1^{2-7,11}. It can be reproduced by peptide A15^B, corresponding to the sequence:



A few sets of experiments, using A15 as analyte, were run on mAb SD6^C surfaces with different densities (8, 1.7 and 0.8 ng/mm²), using peptide concentrations between 1 and 2440 nM and two different buffer flow rates (5 and 60 μ l/min). mAb immobilisation and peptide injection procedures are described in section 4.3.1.1.

1.1.1 High mAb density

In a first approach, a very high mAb surface density (8 ng/mm²) and high A15 concentrations were employed in an attempt to overcome the low responses that were to be expected from the small size of the analyte. Peptide injections were carried out at 5 μ l/min, using the *kinject* mode to avoid sample dispersion at injection plugs, and association and dissociation times were of 7 and 6 minutes, respectively. The surface was regenerated, at the end of each cycle, by a 3-min pulse of 100 mM HCl. The sensorgrams generated under these conditions (Fig. 1.2 A) could not be fitted to the expected 1:1 bimolecular interaction kinetics, as inferred from the high and non-random residuals observed in the dissociation phase (Fig. 1.2 B), and from the concentration-dependence of the association rate constant, k_a (Fig. 1.2 C).

^B Peptides used for optimisation and validation of the SPR experimental set-up were kindly given by Dr. Mari-Luz Valero (Dept. Q.O. - U. B., Barcelona).

^C Monoclonal antibody SD6 is a site-A directed neutralising mAb raised against FMDV C-S8c1; it was kindly supplied by Dr. Nuria Verdaguer and Wendy F. Ochoa (IBMB/CSIC – Barcelona).

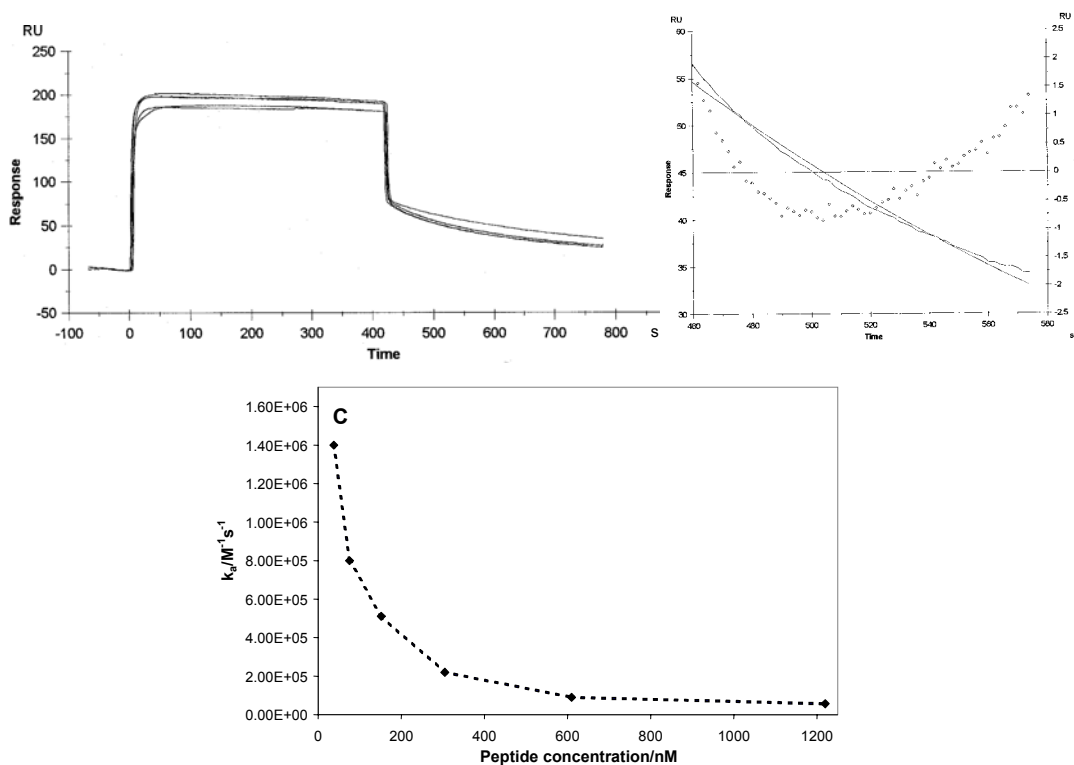


Figure 1. 2 First approach to the SPR kinetic analysis of the interaction between immobilised mAb SD6 and peptide analyte A15: **A**. Experimental sensorgrams; **B**. Distribution of residual data points for the dissociation phase corresponding to $[A15]=310$ nM (detailed view of the experimental and modelled curves); **C**. Variation of k_a with peptide concentration.

The shape of the dissociation curves suggested that some analyte rebinding to the surface was occurring, affecting true kinetics. At the same time, the apparent association rate constant decreased with increasing analyte concentration, *i. e.*, the more peptide was injected, the more difficult became its binding to mAb molecules. So, it appeared that antibody molecules were heterogeneously distributed in the dextran matrix, with different accessibility levels¹². Upon analyte injection, the first peptide molecules would occupy the most accessible mAb receptors and the following ones would have increasing difficulty in reaching free mAb binding sites, such effect becoming larger with higher peptide concentrations. This seemed to be confirmed by the better fit obtained when a *heterogeneous ligand* kinetic model was employed to fit the experimental data (data not shown). This model, however, considers only two different types of ligand, which is most probably far from reality. Since lowering peptide concentration (1 to 50 nM) did not improve the results (data not shown), new conditions were searched in order to obtain experimental data consistent with a langmuirian kinetic behaviour (1:1 bimolecular interaction).

1.1.2 Medium mAb density

The poor results obtained in the previous section were symptomatic of significant heterogeneity in ligand accessibility and orientation. Also, diffusion-controlled delivery of analyte to the most hindered SD6 molecules would be a further cause for the observed deviations. Therefore, a second SD6 surface was prepared with much lower density (1.7 ng/mm²) and another set of injections was run at the same flow rate, spanning peptide concentrations from 1 to 2440 nM. In this case, peptide concentrations below 70 nM were too low for a clear response to be observed, since sensorgrams were hardly distinguished from mere bulk refractive index effects. Higher peptide concentrations led to results better than those described in section 1.1.1, but still presenting some degree of data inconsistency (not shown).

1.1.3 Low mAb density

Further lowering of mAb surface density (to 0.8 ng/mm²), in an attempt to eliminate the non-ideal effects observed so far, did not work either. In fact, this density was seen to be too low for the detection of the FMDV peptides injected, even at analyte concentrations as high as 2.44 μM (not shown).

1.1.4 High buffer flow rate

Since the previous results, all of them obtained at 5 μl/min flow, persistently deviated from the expected behaviour at different mAb surface densities and peptide concentrations, the flow rate seemed an important parameter to manipulate in order to optimise the SPR analysis. Low buffer flow rate could be favouring diffusion-controlled kinetics, affecting true binding constants¹²⁻¹⁴. Therefore, a fourth set of SPR experiments was run, this time using the medium density SD6 surface (1.7 ng/mm²) and high A15 concentrations (152 to 2440 nM), and raising the buffer flow rate to 60 μl/min. Both association and dissociation times were decreased (90 and 240 seconds, respectively) to diminish sample and buffer consumption. Under these experimental conditions, consistent and apparently reliable data were obtained. Experimental and modelled curves were virtually superimposable (Fig. 1.3 A) with a random distribution of residuals within an interval of *ca.* ±0.4 RU (Fig. 1.3 B).

Linearity of k_s versus peptide concentration over the 32-fold concentration range was observed, as required for a concentration-independent k_a (Fig.1.3 C). The *chi*-squared (χ^2) value was smaller than 0.1 and data self-consistency¹⁵ was further confirmed by the total agreement between the values for the equilibrium association constant, K_A , obtained from either the k_a/k_d ratio or from the plot of R_{eq} versus peptide concentration (Fig. 1.3 D)^D.

^D The theoretical basis for SPR kinetic analysis is exposed in section 0.3.

Data analysis produced good quality fits, reproducing the same rate and affinity constants independently from fitting curves globally, locally or with separate association/dissociation phases to the langmuirian kinetics model (Table 1.1).

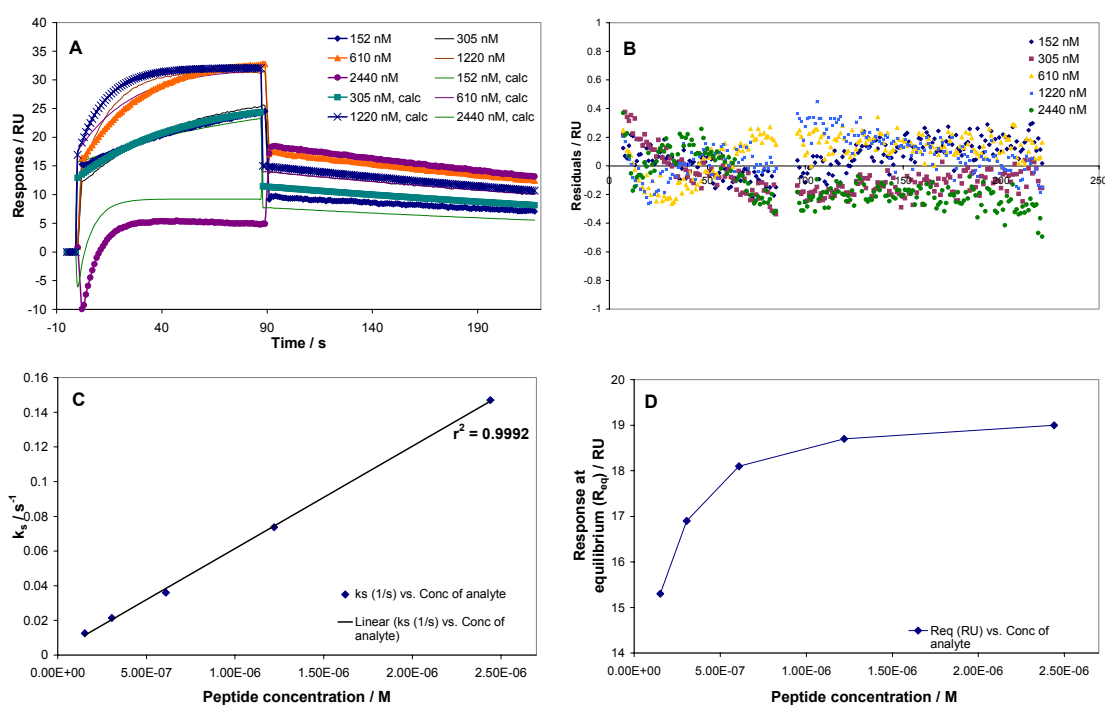


Figure 1.3 Results obtained in the SPR kinetic analysis of the interaction between immobilised mAb SD6 and soluble peptide A15: **A**. Sensorgrams (experimental and modelled); **B**. Distribution of residual data points; **C**. Plot of locally fitted k_s (apparent rate constant, see section 0.3) versus peptide concentration; **D**. Plot of R_{eq} (response at equilibrium) vs. peptide concentration (see section 0.3).

Table 1.1 Quantitative data on the 1:1 langmuirian interaction between immobilised mAb SD6 and soluble peptide A15.

Curve fitting	[peptide]/ nM	$k_a/M^{-1}s^{-1}$	k_d/s^{-1}	K_A/M^{-1}
Global	-	6.2×10^4	2.6×10^{-3}	2.3×10^7
Local, simultaneous k_a/k_d	152	6.0×10^4	2.4×10^{-3}	2.5×10^7
	305	5.8×10^4	2.6×10^{-3}	2.3×10^7
	610	5.9×10^4	2.6×10^{-3}	2.3×10^7
	1220	6.1×10^4	2.7×10^{-3}	2.3×10^7
	2440	6.2×10^4	2.9×10^{-3}	2.1×10^7
Local, separate k_a/k_d	152	6.7×10^4	2.4×10^{-3}	2.8×10^7
	305	6.2×10^4	2.6×10^{-3}	2.4×10^7
	610	5.5×10^4	2.6×10^{-3}	2.1×10^7
	1220	5.8×10^4	2.8×10^{-3}	2.1×10^7
	2440	5.9×10^4	2.7×10^{-3}	2.2×10^7

1.2 Application to the systematic screening of FMDV peptides

1.2.1 Screening of 44 FMDV peptides as antigens towards mAb SD6

Having found suitable experimental conditions for the kinetic analysis of the A15/SD6 interaction, a similar protocol was applied to the systematic screening of 43 other A15 analogues. The antigenicity of these peptides had been previously characterised by competition ELISA⁶, which made them excellent models to evaluate the reliability of our SPR optimised analysis conditions.

An additional peptide, A15scr, with the same constitutive amino acids as A15 but randomly ordered (RAGTATTLADLHYST), was used as a negative control. The scrambled sequence A15scr had no apparent specific binding, but gave rise to a substantial bulk refraction index response (Fig. 1.4 A), as observed for all other peptides analysed. Therefore, the curves for each site A peptide were corrected by subtraction of the corresponding A15scr sensorgrams (Fig. 1.4 B and C). The consistency and accuracy of the fitted kinetic data for the whole set of A15 analogues were in every aspect similar to those described for A15 under the same conditions (Fig. 1.4 D, E and F). The stability of the SD6 surface to the repeated strong acid regeneration cycles allowed the screening of the entire set over the same surface without any detectable loss in mAb activity, thus providing reliable comparison among the different peptides. This is a clear advantage of the present SPR configuration, since in the alternative immobilisation of peptides one cannot control the similarity of the different peptide surfaces. The constants obtained for the interaction between mAb SD6 and the 44 peptides screened are shown in Table 1.2.

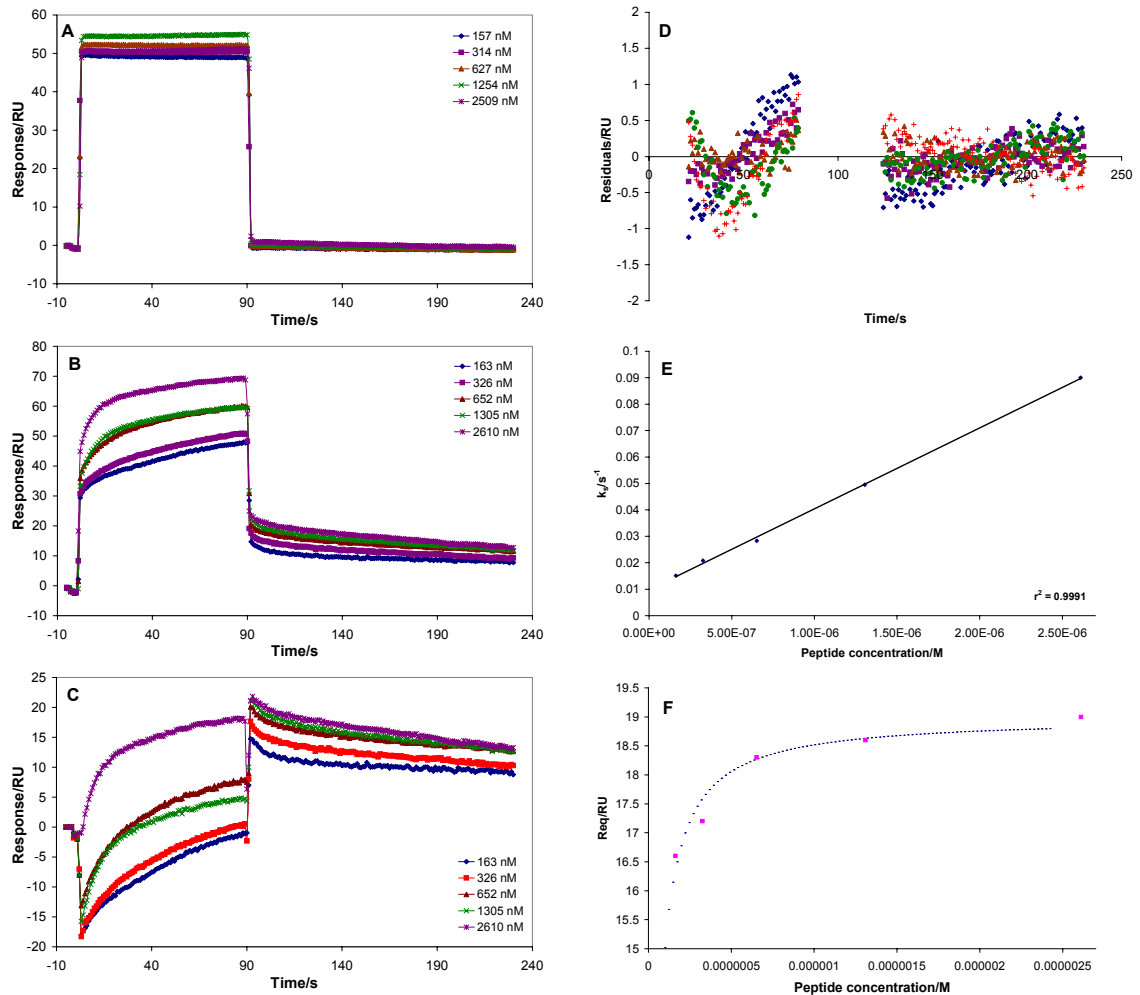


Figure 1.4 **A.** Sensorgrams for the A15scr/SD6 interaction; **B.** Sensorgrams for the interaction between SD6 and an FMDV peptide: A15 (140P); **C.** Sensorgrams of the same interaction as in B, after correction upon subtraction of sensorgrams shown in A; **D.** Residual distribution after fitting sensorgrams C to the 1:1 bimolecular interaction kinetics model; **E.** Linear plot of locally fitted k_s versus peptide concentration; **F.** Plot of locally fitted R_{eq} versus peptide concentration (for comparison between the association equilibrium constants as obtained from this plot or from the k_a/k_d ratio).

Table 1.2 Kinetic data^a of the interactions between mAb SD6 and 44 site A peptides^b.

PEPTIDE	$k_a/M^{-1}s^{-1}$	k_d/s^{-1}	K_A/M^{-1}	ELISA	PEPTIDE	$k_a/M^{-1}s^{-1}$	k_d/s^{-1}	K_A/M^{-1}	ELISA
A15	7.3×10^4	1.4×10^{-3}	5.4×10^7		A15(148S)	9.4×10^4	6.7×10^{-3}	1.4×10^7	
A15(137P)	5.8×10^4	1.9×10^{-3}	3.1×10^7		A15(138D)	ni	ni	ni	
A15(138P)	ni	ni	ni		A15(138E)	ni	ni	ni	
A15(139P)	ni	ni	ni		A15(138F)	8.6×10^4	3.9×10^{-3}	2.2×10^7	
A15(140P)	7.4×10^4	2.1×10^{-3}	3.5×10^7		A15(138K)	ni	ni	ni	
A15(141P)	ni	ni	ni		A15(138R)	ni	ni	ni	
A15(142P)	ni	ni	ni			1.3×10^5	7.1×10^{-3}	1.8×10^7	
A15(143P)	ni	ni	ni		A15(138Y)	2.3×10^5	8.8×10^{-3}	2.6×10^7	
A15(144P)	ni	ni	ni		A15(145D)	ni	ni	ni	
A15(145P)	ni	ni	ni		A15(145E)	5.3×10^4	4.1×10^{-3}	1.3×10^7	
A15(146P)	ni	ni	ni		A15(145F)	ni	ni	ni	
A15(147P)	ni	ni	ni		A15(145I)	ni	ni	ni	
A15(148P)	6.6×10^4	6.2×10^{-2}	1.1×10^7		A15(145K)	4.5×10^4	4.1×10^{-3}	1.1×10^7	
A15(137S)	1.2×10^5	3.5×10^{-3}	3.5×10^7		A15(145R)	1.4×10^4	9.7×10^{-3}	1.4×10^6	
A15(138S)	1.1×10^5	1.2×10^{-2}	8.8×10^6		A15(147A)	9.2×10^4	2.1×10^{-3}	4.4×10^7	
A15(140S)	1.5×10^5	8.6×10^{-4}	1.8×10^8		A15(147D)	ni	ni	ni	
A15(141S)	4.5×10^4	2.6×10^{-3}	1.8×10^7		A15(147E)	6.7×10^4	3.1×10^{-3}	2.2×10^7	
A15(142S)	6.1×10^4	5.6×10^{-3}	1.1×10^7		A15(147G)	3.2×10^5	6.1×10^{-3}	3.7×10^7	
A15(143S)	ni	ni	ni		A15(147K)	6.6×10^4	3.4×10^{-3}	2.0×10^7	
A15(144S)	ni	ni	ni		A15(147N)	4.6×10^4	5.0×10^{-3}	9.2×10^6	
A15(145S)	4.0×10^4	5.1×10^{-3}	7.8×10^6		A15(147R)	7.9×10^4	3.5×10^{-3}	2.3×10^7	
A15(147S)	1.3×10^4	1.1×10^{-2}	1.2×10^6		A15(147V)	9.2×10^4	6.6×10^{-3}	1.4×10^7	

^a corrected for non-specific binding; ^b qualitative relative antigenicities from ELISA competition assays are represented, with a black box corresponding to $IC_{50} > 100$, a dark grey box to $IC_{50} = 30$ to 100, a light grey box to $IC_{50} = 5$ to 30 and a white box to $IC_{50} < 5$. "ni" - no measurable interaction.

Table 1.2 also includes previous data from enzyme-linked immunosorbent assays (ELISA)⁶. These data had been expressed as IC₅₀ values (competitor peptide concentration giving a 50 % drop in maximal absorbance), normalised to the IC₅₀ of peptide A15 (see section 4.3.2). A general agreement between both SPR and ELISA techniques was observed, thus supporting the reliability of the functional characterisation of small antigenic FMDV peptides using SPR.

1.2.2 Reproducibility in the SPR constants measured on the SD6 surface

Although systematic repetition of assays for every analyte was not possible, given the large number of peptides, the reproducibility of our SPR analysis was nevertheless assessed by repeated injection of a representative sub-set of peptides. Six A15 analogues were independently analysed six times under similar conditions, with the results shown in Table 1.3. Standard deviations of the measured kinetic parameters oscillate between 2 and 11% of the mean value, which is quite good considering the small size of the analytes. A sole exception was seen with k_d for the SD6/A15(137I) complex (SD=20%), which is not surprising given the very low dissociation rate observed for this complex, making it more prone to be affected by experimental error.

Table 1.3 Reproducibility in kinetic SPR analyses of SD6/peptide interactions (six assays per peptide).

Peptide	$k_a/M^{-1}s^{-1}$	k_d/s^{-1}	Peptide	$k_a/M^{-1}s^{-1}$	k_d/s^{-1}
A15 (137I)	1.0×10^5	6.5×10^{-4}	A15 (145E)	2.88×10^4 (*)	3.74×10^{-3} (*)
	9.7×10^4	4.7×10^{-4}		4.69×10^4	4.13×10^{-3}
	9.1×10^4	4.3×10^{-4}		5.76×10^4	3.63×10^{-3}
	9.6×10^4	5.1×10^{-4}		4.82×10^4	4.23×10^{-3}
	8.7×10^4 (*)	8.0×10^{-5} (*)		6.23×10^4	4.28×10^{-3}
	9.3×10^5 (*)	2.7×10^{-4} (*)		5.21×10^4	4.15×10^{-3}
<i>mean±SD</i>	$(9.6 \pm 0.4) \times 10^4$	$(5 \pm 1) \times 10^{-4}$	<i>mean±SD</i>	$(5.3 \pm 0.6) \times 10^4$	$(4.1 \pm 0.3) \times 10^{-3}$
A15 (138K)	n.i.	n.i.	A15 (145K)	2.87×10^4 (*)	4.67×10^{-3} (*)
	n.i.	n.i.		4.15×10^4	4.55×10^{-3}
	n.i.	n.i.		4.86×10^4	4.00×10^{-3}
	n.i.	n.i.		4.40×10^4	3.90×10^{-3}
	n.i.	n.i.		4.52×10^4	4.07×10^{-3}
	n.i.	n.i.		2.45×10^4	3.99×10^{-3}
<i>mean±SD</i>	-	-	<i>mean±SD</i>	$(4.5 \pm 0.3) \times 10^4$	$(4.1 \pm 0.3) \times 10^{-3}$
A15(148I)	1.22×10^5	1.90×10^{-3}	A15(145R)	2.09×10^4 (*)	9.65×10^{-3} (*)
	9.33×10^4 (*)	1.98×10^{-3} (*)		3.05×10^4 (*)	5.40×10^{-3} (*)
	1.19×10^5	2.43×10^{-3}		1.44×10^4	9.01×10^{-3}
	7.24×10^4	2.44×10^{-3}		1.38×10^4	9.46×10^{-3}
	1.00×10^5	1.88×10^{-3}		1.37×10^4	1.03×10^{-3}
	1.13×10^5	2.17×10^{-3}		1.37×10^4	1.01×10^{-3}
<i>mean±SD</i>	$(1.1 \pm 0.1) \times 10^5$	$(2.1 \pm 0.2) \times 10^{-3}$	<i>mean±SD</i>	$(1.39 \pm 0.03) \times 10^4$	$(9.7 \pm 0.6) \times 10^{-3}$

(*) data was not considered for calculating mean and standard deviation values.

1.3 Use of other site A-directed monoclonal antibodies

A desirable general applicability of our direct kinetic SPR antigenic analysis of small site A peptides would obviously require not only the ability to distinguish between different analytes (antigens) but also between different receptors (antibodies). Therefore, it was decided to adapt the procedure to a new mAb, 4C4^E, as the immobilised receptor.

1.3.1 Adaptation of the experimental set-up to a new mAb

In order to obtain good quality data with mAb 4C4, slight changes had to be introduced in the protocols of SPR analysis previously described for mAb SD6. MAb 4C4 coupled more efficiently to the dextran matrix under the same conditions employed for the immobilisation of SD6: immobilisation levels had to be therefore adjusted by dilution of the mAb solution, to achieve a final surface densities of ca. 1600 RU (1.6 ng/mm²).

Also, it was observed that 4C4 surfaces were not suitably regenerated with hydrochloric acid. A clear symptom for this problem was that sensorgrams from the same 4C4 surface showed an increase in baseline response and a concomitant decrease in signal for identical A15 concentrations over repetitive cycles (not shown). Alternative regeneration procedures, using other acids (phosphoric or formic) or bases (10 mM glycine, pH 12 or 10 mM sodium hydroxide) were tested and sodium hydroxide was found to be the most efficient regenerating agent.

Further, while for SD6 the optimal analyte concentration range was generally between ca. 75 and 1250 nM, for 4C4 saturation was already reached at concentrations above 600 nM (not shown). This observation suggested that mAb 4C4 possessed higher affinity than SD6 towards the site A peptides, which was later confirmed upon peptide analysis on 4C4 surfaces (see following section).

1.3.2 Screening of 44 FMDV peptides as antigens towards mAb 4C4

A systematic screening similar to that described in section 1.2.1 was performed on a 4C4 surface (Fig. 1.5). Surface mAb density and injection parameters were quite the same, with the only difference being the peptide concentrations used (from 35 to 1250 nM). The kinetic data were fitted as before, generally displaying identical accuracy and consistency levels. Once more, the global agreement between SPR-derived affinities and previous ELISA data was remarkable and further validated the experimental SPR set-up (Table 1.4).

^E mAb 4C4 is a site-A directed, anti-FMDV neutralising antibody, raised against strain C₁-Brescia; it was kindly supplied by Dr. Nuria Verdaguer and Ms. Wendy F. Ochoa (IBMB/CSIC – Barcelona, Spain).

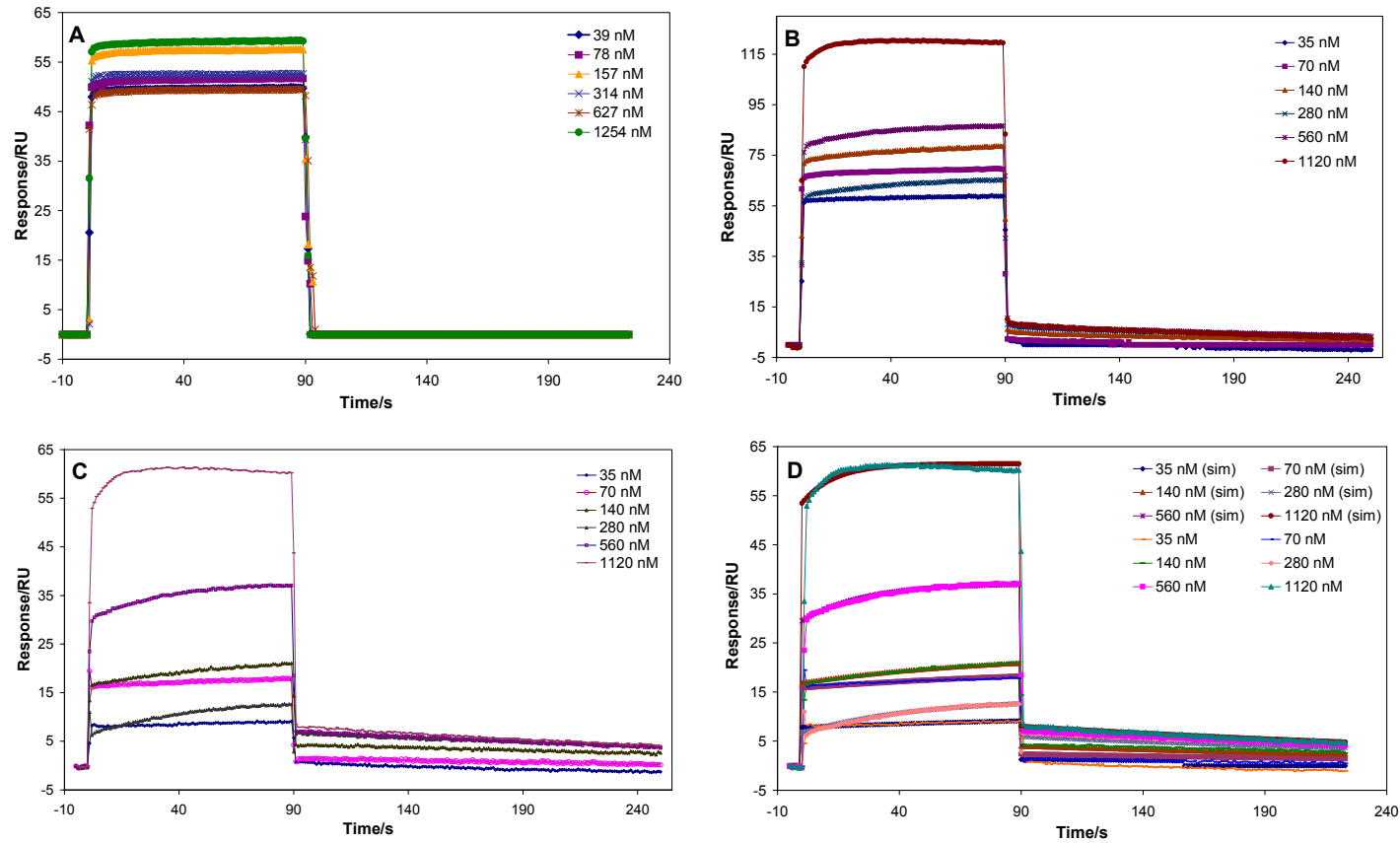


Figure 1.5 A. Binding curves for non-specific peptide A15scr on a mAb 4C4 surface. The remaining plots are sensorgrams for binding of peptide A15(142S) to mAb 4C4: **B.** Raw data; **C.** After correction for non-specific binding; **D.** Overlay plot of experimental (corrected) and simulated (sim) sensorgrams. [Note: higher total (R_{tot}) responses correspond to higher peptide concentrations, except for 280 nM peptide injection (second smaller response) which presented a lower bulk RI jump].

Table 1.4 Kinetic data^a of the interactions between mAb 4C4 and 44 site A peptides^b.

PEPTIDE	$k_a/M^{-1}s^{-1}$	k_d/s^{-1}	K_A/M^{-1}	ELISA	PEPTIDE	$k_a/M^{-1}s^{-1}$	k_d/s^{-1}	K_A/M^{-1}	ELISA
A15	3.8×10^5	1.9×10^{-3}	1.9×10^8		A15(148S)	3.0×10^5	7.9×10^{-3}	3.8×10^7	
A15(137P)	1.2×10^5	6.1×10^{-4}	2.0×10^8		A15(138D)	n.i.	n.i.	n.i.	■
A15(138P)	4.1×10^5	5.1×10^{-2}	8.0×10^6	■	A15(138E)	n.i.	n.i.	n.i.	■
A15(139P)	n.i.	n.i.	n.i.	■	A15(138F)	5.5×10^5	5.7×10^{-3}	9.8×10^7	
A15(140P)	1.9×10^5	1.9×10^{-3}	1.0×10^8		A15(138K)	3.5×10^5	2.3×10^{-2}	1.5×10^7	■
A15(141P)	n.i.	n.i.	n.i.	■	A15(138R)	1.4×10^5	1.9×10^{-2}	7.4×10^6	■
A15(142P)	n.i.	n.i.	n.i.	■	A15(138V)	2.7×10^5	1.4×10^{-3}	2.0×10^8	
A15(143P)	n.i.	n.i.	n.i.	■	A15(138Y)	4.0×10^5	1.3×10^{-3}	3.0×10^8	
A15(144P)	n.i.	n.i.	n.i.	■	A15(145D)	n.i.	n.i.	n.i.	■
A15(145P)	n.i.	n.i.	n.i.	■	A15(145E)	1.5×10^5	2.2×10^{-3}	6.9×10^7	
A15(146P)	n.i.	n.i.	n.i.	■	A15(145F)	1.4×10^5	5.1×10^{-3}	2.7×10^7	■
A15(147P)	n.i.	n.i.	n.i.	■	A15(145I)	1.7×10^5	6.4×10^{-3}	2.7×10^7	■
A15(148P)	1.6×10^5	1.4×10^{-2}	1.2×10^7		A15(145K)	2.5×10^5	2.3×10^{-3}	1.1×10^8	
A15(137S)	1.7×10^5	3.0×10^{-3}	5.6×10^7		A15(145R)	6.6×10^4	5.9×10^{-3}	1.1×10^7	
A15(138S)	2.5×10^5	2.2×10^{-3}	1.1×10^8		A15(147A)	n.i.	n.i.	n.i.	■
A15(140S)	2.5×10^5	2.4×10^{-3}	1.1×10^8		A15(147D)	n.i.	n.i.	n.i.	■
A15(141S)	1.2×10^5	3.5×10^{-3}	3.2×10^7		A15(147E)	n.i.	n.i.	n.i.	■
A15(142S)	6.3×10^4	3.8×10^{-3}	1.6×10^7		A15(147G)	n.i.	n.i.	n.i.	■
A15(143S)	n.i.	n.i.	n.i.	■	A15(147K)	n.i.	n.i.	n.i.	■
A15(144S)	n.i.	n.i.	n.i.	■	A15(147N)	n.i.	n.i.	n.i.	■
A15(145S)	3.8×10^5	7.6×10^{-3}	5.1×10^7	■	A15(147R)	n.i.	n.i.	n.i.	■
A15(147S)	n.i.	n.i.	n.i.	■	A15(147V)	1.4×10^5	5.6×10^{-2}	2.5×10^6	■

^a corrected for non-specific binding; ^b qualitative relative antigenicities from ELISA competition assays are represented, with a black box corresponding to $IC_{50} > 100$, a dark grey box to $IC_{50} = 30$ to 100, a light grey box to $IC_{50} = 5$ to 30 and a white box to $IC_{50} < 5$. “ni” - no measurable interaction.

1.3.3 Reproducibility in the constants measured on the 4C4 surface

As already described in section 1.2.1, reproducibility of the SPR-measured constants was evaluated through repetitive analyses of a small set of site A peptides. Again, six peptides were independently analysed six times on a mAb 4C4 surface. Results for mAb 4C4 are presented in Table 1.5 and show very good reproducibility, with standard deviations less than 9% of the mean values.

Table 1.5 Reproducibility in kinetic SPR analysis of 4C4/peptide interactions (six assays per peptide).

Peptide	$k_a/M^{-1}s^{-1}$	k_d/s^{-1}	$k_a/M^{-1}s^{-1}$	k_d/s^{-1}
A15(138D)	n.i.	n.i.	1.06×10^5 (*)	2.16×10^{-2} (*)
	n.i.	n.i.	1.46×10^5	1.94×10^{-2}
	n.i.	n.i.	1.45×10^5	1.88×10^{-2}
	n.i.	n.i.	1.51×10^5	2.08×10^{-2}
	n.i.	n.i.	1.42×10^5	1.94×10^{-2}
	n.i.	n.i.	1.39×10^5	1.88×10^{-2}
mean \pm SD	–	–	mean \pm SD $(1.45 \pm 0.05) \times 10^5$	$(1.94 \pm 0.07) \times 10^{-2}$
A15(138F)	5.54×10^5	5.06×10^{-3}	2.56×10^5	6.59×10^{-4}
	6.00×10^5	6.23×10^{-3}	2.90×10^5	1.34×10^{-3}
	4.70×10^5	5.44×10^{-3}	2.49×10^5	1.15×10^{-3}
	5.68×10^5	5.55×10^{-3}	2.67×10^5	1.34×10^{-3}
	5.70×10^5	6.04×10^{-3}	2.72×10^5	1.60×10^{-3}
	4.90×10^5 (*)	1.16×10^{-3} (*)	2.83×10^5	1.62×10^{-3}
mean \pm SD	$(5.5 \pm 0.5) \times 10^5$	$(5.7 \pm 0.5) \times 10^{-3}$	mean \pm SD $(2.7 \pm 0.2) \times 10^5$	$(1.4 \pm 0.2) \times 10^{-3}$
A15(138K)	3.05×10^5	2.35×10^{-2}	4.46×10^5 (*)	1.41×10^{-3} (*)
	3.62×10^5	2.33×10^{-2}	3.99×10^5	1.32×10^{-3}
	3.74×10^5	2.33×10^{-2}	4.05×10^5	1.12×10^{-3}
	3.78×10^5	2.40×10^{-2}	3.82×10^5	1.41×10^{-3}
	3.38×10^5	2.25×10^{-2}	3.80×10^5	1.48×10^{-3}
	4.65×10^5 (*)	2.25×10^{-2} (*)	3.82×10^5	1.34×10^{-3}
mean \pm SD	$(3.5 \pm 0.3) \times 10^5$	$(2.32 \pm 0.06) \times 10^{-2}$	mean \pm SD $(4.0 \pm 0.3) \times 10^5$	$(1.3 \pm 0.1) \times 10^{-3}$
A15(138R)	n.i.	n.i.	1.06×10^5 (*)	2.16×10^{-2} (*)
	n.i.	n.i.	1.46×10^5	1.94×10^{-2}
	n.i.	n.i.	1.45×10^5	1.88×10^{-2}
	n.i.	n.i.	1.51×10^5	2.08×10^{-2}
	n.i.	n.i.	1.42×10^5	1.94×10^{-2}
	n.i.	n.i.	1.39×10^5	1.88×10^{-2}
mean \pm SD	–	–	mean \pm SD $(1.45 \pm 0.05) \times 10^5$	$(1.94 \pm 0.07) \times 10^{-2}$
A15(138V)	5.54×10^5	5.06×10^{-3}	2.56×10^5	6.59×10^{-4}
	6.00×10^5	6.23×10^{-3}	2.90×10^5	1.34×10^{-3}
	4.70×10^5	5.44×10^{-3}	2.49×10^5	1.15×10^{-3}
	5.68×10^5	5.55×10^{-3}	2.67×10^5	1.34×10^{-3}
	5.70×10^5	6.04×10^{-3}	2.72×10^5	1.60×10^{-3}
	4.90×10^5 (*)	1.16×10^{-3} (*)	2.83×10^5	1.62×10^{-3}
mean \pm SD	$(5.5 \pm 0.5) \times 10^5$	$(5.7 \pm 0.5) \times 10^{-3}$	mean \pm SD $(2.7 \pm 0.2) \times 10^5$	$(1.4 \pm 0.2) \times 10^{-3}$
A15(138Y)	3.05×10^5	2.35×10^{-2}	4.46×10^5 (*)	1.41×10^{-3} (*)
	3.62×10^5	2.33×10^{-2}	3.99×10^5	1.32×10^{-3}
	3.74×10^5	2.33×10^{-2}	4.05×10^5	1.12×10^{-3}
	3.78×10^5	2.40×10^{-2}	3.82×10^5	1.41×10^{-3}
	3.38×10^5	2.25×10^{-2}	3.80×10^5	1.48×10^{-3}
	4.65×10^5 (*)	2.25×10^{-2} (*)	3.82×10^5	1.34×10^{-3}
mean \pm SD	$(3.5 \pm 0.3) \times 10^5$	$(2.32 \pm 0.06) \times 10^{-2}$	mean \pm SD $(4.0 \pm 0.3) \times 10^5$	$(1.3 \pm 0.1) \times 10^{-3}$

(*) data was not considered for calculating mean and standard deviation values.

1.4 Probing subtle differences in peptide and mAb behaviour by SPR

Comparison of the results in sections 1.2 and 1.3 leads to the immediate conclusion that not only the different features of the peptides analysed can be distinguished through SPR, but also distinct mAb “personalities” can be appreciated.

Peptides screened on the same mAb surface are mainly distinguished by their dissociation rate constants. A closer look into Tables 1.2 or 1.4 shows that k_a varies over a 10-fold range, while k_d varies over a 100-fold range. This observation has already been reported^{16,17} and it has been proposed that the biologically relevant SPR-derived parameter is, in fact, k_d , since it is a measure of the life-time of the ligand-receptor complex. Correlations between dissociation rate constants and neutralisation have also been found¹⁸.

On the other hand, comparison of data from the two mAb surfaces seems to suggest that each antibody has its own “avidity range”, *i. e.*, its own range of association rate constants, which provide a measure of the accessibility of a particular paratope towards similar antigens. Thus, while average k_a for SD6 is $7.9 \times 10^4 \text{ M}^{-1}\text{s}^{-1}$, for mAb 4C4 it is $2.4 \times 10^5 \text{ M}^{-1}\text{s}^{-1}$, a three-fold increase.

The validity of the SPR approach for the screening of antigenic site A peptides is better illustrated in Fig. 1.6, which shows the good correlation between antigenicity data measured with SPR and previous results from competition ELISA. Also, the distinct recognition requirements imposed by different antibodies is clearly demonstrated upon comparison of Figs. 1.6 A and 1.6 B, particularly in what concerns recognition of A15 analogues displaying mutations at position 147 (corresponding to a leucine in the native sequence). This provides further proof of the suitability of SPR to the functional study of antigenic determinants in viral epitopes using synthetic peptides.

1.5 Validity of the experimental kinetic constants

Evaluation of mass-transport influence on kinetic data is often advisable. Tests should include analysis over a concentration range from 0.1 to $10 K_D$, variation of the buffer flow rate and also variation of the binding capacity using different surface densities¹³⁻¹⁵. In this work, consistent results were observed for peptides analysed over a 30-fold concentration range, from as high as $10 K_D$ down to *ca.* 40 nM. The 0.1 K_D condition was possible only for peptides with K_D values at or above the μM level, since response could not be accurately measured at lower peptide concentrations.

Mass-transport effects were evaluated on peptide A15 at two different buffer flow rates (2 and 60 $\mu\text{l}/\text{min}$) and three different surface capacities (*ca.* 0.5, 1.6 and 2.5 ng/mm^2) as shown in Table 1.6. Binding was not measurable at the lowest density surfaces, as expected from both previous results (section 1.1) and small size of the analytes.

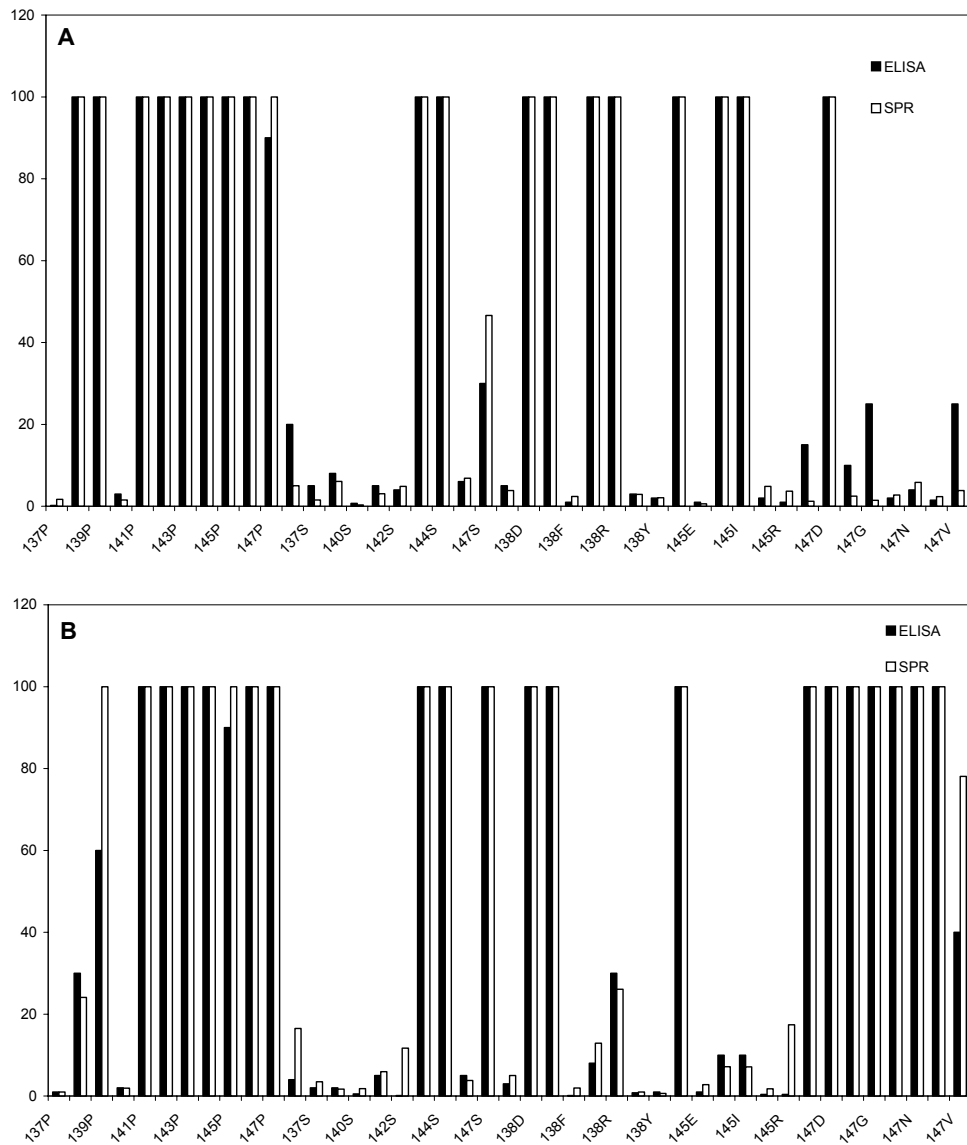


Figure 1. 6 Comparison of SPR [$\text{relative } K_D = K_D(\text{peptide X})/K_D(\text{peptide A15})$] and ELISA [$\text{relative } IC_{50} = IC_{50}(\text{peptide X})/IC_{50}(\text{peptide A15})$] affinity data for the 43 variants of A15 towards: **A.** mAb SD6; **B.** mAb 4C4. Peptides displaying IC_{50} or K_D values too high to be accurately measured are represented by bars truncated at 100. In the horizontal axis are represented the A15 analogues screened, with the number corresponding to the A15 position replaced and the letter corresponding to the capital case code of the amino acid residue introduced at that position (*only half of the peptide labels are shown for simplicity*).

Higher densities did not show important differences in kinetic rate constants, with all data sets giving best fits to the 1:1 langmuirian interaction model. Despite deviations observed when the smaller buffer flow rate was employed, these hardly affected the magnitude of the kinetic rate constants or the quality of the fitted data.

Table 1.6 Kinetic data for the mAb SD6/peptide A15 and mAb 4C4/peptide A15 binding interactions under different buffer flow rate and surface density conditions.

Buffer flow rate ($\mu\text{L}/\text{min}$)	SD6/ng.mm ⁻²			4C4/ng.mm ⁻²		
	0.5	1.6	2.5	0.4	1.7	2.7
2		$k_a=5.9\times 10^4\text{M}^{-1}\text{s}^{-1}$	$k_a=9.0\times 10^4\text{M}^{-1}\text{s}^{-1}$		$k_a=2.1\times 10^5\text{M}^{-1}\text{s}^{-1}$	$k_a=2.6\times 10^5\text{M}^{-1}\text{s}^{-1}$
	*	$k_d=1.3\times 10^{-3}\text{s}^{-1}$	$k_d=1.2\times 10^{-3}\text{s}^{-1}$	*	$k_d=1.6\times 10^{-3}\text{s}^{-1}$	$k_d=8.4\times 10^{-4}\text{s}^{-1}$
		$\chi^2=0.3$	$\chi^2=1.1$		$\chi^2=2$	$\chi^2=0.4$
60		$k_a=7.3\times 10^4\text{M}^{-1}\text{s}^{-1}$	$k_a=1.1\times 10^5\text{M}^{-1}\text{s}^{-1}$		$k_a=3.8\times 10^5\text{M}^{-1}\text{s}^{-1}$	$k_a=5.0\times 10^5\text{M}^{-1}\text{s}^{-1}$
	*	$k_d=1.4\times 10^{-3}\text{s}^{-1}$	$k_d=1.8\times 10^{-3}\text{s}^{-1}$	*	$k_d=1.9\times 10^{-3}\text{s}^{-1}$	$k_d=2.0\times 10^{-3}\text{s}^{-1}$
		$\chi^2=0.2$	$\chi^2=2.2$		$\chi^2=1.0$	$\chi^2=0.5$

* no reliable measurements at this surface density.

Mass-transport limitations are not usually dramatic for small analytes and can be avoided with careful experimental set-ups, where high buffer flow rates and low surface densities are key features. However, even when careful experimental design is applied and apparently consistent data is obtained, one cannot rule out the possibility of diffusion-controlled kinetics. Hence, the SPR-derived kinetic rate constants cannot be considered as absolutely “true” values. Further, one cannot fully compare the events taking place at the biosensor surface, where the biological receptor is immobilised, with those occurring in solution or in physiologic media. Although agreement with ELISA experiments provides a valuable check for the reliability of biosensor data, one cannot write off the possibility that mass-transport affects actual k_a and k_d values by a similar factor, thus providing thermodynamic constants apparently consistent with equilibrium experiments. Nevertheless, the real usefulness of the SPR technology lies in the comparative analysis of the kinetic behaviour of analogous analytes screened under the same experimental conditions and this was the purpose of the present work.

1.6 Relevance of the SPR data for FMDV studies

Antigenic site A is a key component of the immune response against FMDV, and some of its constituent amino acid residues play a decisive role in the mechanisms of FMDV escape under immune pressure¹⁹. The involvement of the RGD tripeptide motif in both antibody and host cell recognition, as well as the importance of key adjacent residues such as Leu 144 and Leu 147 were well-established in previous studies, where site A variant peptides proved very useful in probing the antigenic structure of this site^{5,6,11,20}. Since only equilibrium data had been reported so far, the dynamic aspects of site A peptide-antibody interactions remained unexplored and real-time biospecific SPR analysis seemed the right tool to perform such an exploration. Forty-three analogues of the site A reference peptide A15 (from the C-Sc8c1 FMDV clone) were chosen to show how structural variation within site A can be correlated with and adequately explained by kinetic SPR data.

The choice of peptides focused on several structural features of antigenic site A. A *proline scan* was first performed from residues 137 to 148 of the GH loop. The well-known structure-disrupting effect of Pro was reflected in a complete absence of measurable binding when Pro was replacing residues within the RGD triplet or the following short helical stretch at Asp 142 – Leu 147^{5,6}. Replacement at the N-terminal region did not affect binding in positions 137 and 140, but produced a slight decrease and a significant loss in antigenicity for positions 138 and 139, respectively. This agrees with reported observations that Ser 139 participates in important polar interactions⁶ in which Pro is unable to engage. Next, a *serine scan* was performed, given the striking preservation of antigenicity in site A variants having Ser at critical positions⁶. Ser replacements at the 137 – 142 region are in general well-tolerated, including positions 141 and 142, corresponding to Arg and Gly of the RGD motif. On the other hand, changes at either Asp 143, Leu 144 and Leu 147 were clearly detrimental to recognition, a result which can be explained by (i) the role of the Asp residue of the RGD motif in antibody recognition and (ii) the fact that both Leu 144 and Leu 147 are involved in hydrophobic interactions in all available three-dimensional structures of peptide A15 – antibody complexes^{5,6}.

A third group of variant peptides included replacements at positions 138, 145 and 147 to illustrate the subtle effects that structural variation can bring about in antibody recognition. For instance, replacements with charged basic (Arg, Lys) residues at Ala 138 are better tolerated by mAb 4C4 than by SD6. This is in agreement with the higher percentage of residue contact observed for the latter mAb in the crystal structure of A15 – antibody complexes⁶. Non-polar aliphatic or aromatic amino acids seem to be acceptable by both mAbs at this position. Changes at position 145 (Ala) are similarly interesting. While SD6 does not recognise peptides with non-polar replacements, 4C4 easily binds the same mutated peptides. Even more striking is the reactivity of both mAbs with the Glu-replaced peptide, whereas the Asp mutation is not recognised. Finally, position 147 provides the more critical differentiation between both mAbs assayed: while SD6 is quite tolerant to mutations (except Asp), 4C4 is extremely sensitive to changes at this position.

References

- 1 Fägerstam, L. G., Frostell-Karlsson, A., Karlsson, R., Persson, B. and Rönnberg, I. (1992) Biospecific interaction analysis using surface plasmon resonance detection applied to kinetic, binding site and concentration analysis, *J. Chromatogr.* **597**, 397.
- 2 Van Regenmortel, M. H. V., Altschuh, D., Pellequer, J. L., Richalet-Sécordel, P., Saunal, H., Wiley, J. A., Zeder-Lutz, G. (1994) Analysis of viral antigens using biosensor technology. *Methods: A Comp. Meth. Enzymol.* **6**, 177.
- 3 Carreño, C., Roig, X., Camarero, J., Mateu, M. G., Domingo, E., Giral, E., Andreu, D. (1992) Studies on antigenic variability of C strains of foot-and-mouth disease virus by means of synthetic peptides and monoclonal antibodies. *Int. J. Peptide Protein Res.* **39**, 41.
- 4 Feigelstock, D. A., Mateu, M. G., Valero, M. L., Andreu, D., Domingo, E., Palma, E. L. (1996) Emerging foot-and-mouth disease virus variants with antigenically critical amino acid substitutions predicted by model studies using reference viruses. *Vaccine* **14**, 97.
- 5 Verdaguer, N., Mateu, M. G., Andreu, D., Giral, E., Domingo, E., Fita, I. (1995) Structure of the major antigenic loop of foot-and-mouth disease virus complexed with a neutralizing antibody: direct involvement of the Arg-Gly-Asp motif in the interaction. *EMBO J.* **14**, 1690.
- 6 Verdaguer, N., Sevilla, N., Valero, M. L., Stuart, D., Brocchi, E., Andreu, D., Giral, E., Domingo, E., Mateu, M. G., Fita, I. (1998) A similar pattern of interaction for different antibodies with a major antigenic site of foot-and-mouth disease virus: implications for intratypic antigenic variation. *J. Virol.* **72**, 739.
- 7 Mateu, M.G., Andreu, D., Carreño, C., Roig, X., Cairó, J. J., Camarero, J. A., Giral, E. and Domingo, E. (1992) Non-additive effects of multiple amino acid substitutions on antigen-antibody recognition. *Eur. J. Immunol.* **22**, 1385.
- 8 Karlsson, R., Ståhlberg R. (1995) Surface plasmon resonance detection and multispot sensing for direct monitoring of interactions involving low-molecular-weight analytes and for determination of low affinities. *Anal. Biochem.* **228**, 274.
- 9 Karlsson, R. (1994) Real-time competitive kinetic analysis of interactions between low-molecular-weight ligands in solution and surface-immobilized receptors. *Anal. Biochem.* **221**, 142.
- 10 Abbas, A. K., Lichtman, A. H. and Pober, J. S. "Cellular and molecular immunology", 3rd edition; W. B. Saunders Co., New York (1997).
- 11 Mateu, M. G., Valero, M. L., Andreu, D. and Domingo, E. (1996) Systematic replacement of amino acid residues within an Arg-Gly-Asp-containing loop of foot-and-mouth disease virus and effect on cell recognition. *J. Biol. Chem.* **271**, 12814.
- 12 O'Shannessy, D. J., Winzor, D. J. (1996) Interpretation of deviations to pseudo-first-order kinetic behavior in the characterization of ligand binding by biosensor technology. *Anal. Biochem.* **236**, 275.
- 13 Schuck, P. (1997) Use of surface plasmon resonance to probe the equilibrium and dynamic aspects of interactions between biological macromolecules. *Ann. Rev. Biophys. Biomol. Struct.* **26**, 541.
- 14 Schuck, P. (1997) Reliable determination of binding affinity and kinetics using surface plasmon resonance biosensors. *Curr. Op. Biotechnol.* **8**, 498.
- 15 Shuck, P. and Minton, A. P. (1996) Kinetic analysis of biosensor data: elementary tests for auto-consistency. *Trends Biochem. Sci.* **21**, 458-460.
- 16 Altschuh, D., Dubs, M. C., Weiss, E., Zeder-Lutz, G., Van Regenmortel, M. H. V. (1992) Determination of kinetic constants for the interactions between a monoclonal antibody and peptides using surface plasmon resonance. *Biochemistry* **31**, 6298.
- 17 England, P., Brégère, F. and Bedouelle, H. (1997) Energetic and kinetic contributions of contact residues of antibody D1.3 in the interaction with lysozyme. *Biochemistry* **36**, 164.
- 18 VanCott, T. C., Bethke, F. R., Polonis, V. R., Gorny, M. K., Zolla-Pazner, S., Redfield, R. R. and Birx, D. L. (1994) Dissociation rate of antibody-gp120 binding interactions is predictive of V3-mediated neutralization of HIV-1. *J. Immunol.* **153**, 449.
- 19 Martínez, M. A., Hernández, J., Piccone, M. E., Palma, E. L., Domingo, E., Knowles, E. and Mateu, M. G. (1991) Two mechanisms of antigenic diversification of foot-and-mouth disease virus. *Virology* **184**, 695.
- 20 Hernández, J., Valero, M. L., Andreu, D., Domingo, E. and Mateu, M. G. (1996) Antibody and host cell recognition of foot-and-mouth disease virus (serotype C) cleaved at the Arg-Gly-Asp (RGD) motif: a structural interpretation. *J. Gen. Virol.* **77**, 257.